



OPEN

SUBJECT AREAS:
NEOPLASM STAGING
CANCER IMAGINGReceived
31 July 2014Accepted
23 October 2014Published
10 November 2014Correspondence and
requests for materials
should be addressed to
G.-B.C. (cgbd@126.
com)* These authors
contributed equally to
this article.

Predicting Subtypes of Thymic Epithelial Tumors Using CT: New Perspective based on a Comprehensive Analysis of 216 Patients

Yu-Chuan Hu^{1*}, Lang Wu^{2*}, Lin-Feng Yan^{1*}, Wen Wang³, Shu-Mei Wang⁴, Bao-Ying Chen¹, Gang-Feng Li¹, Bei Zhang¹ & Guang-Bin Cui¹

¹Department of Radiology, Tangdu Hospital, Fourth Military Medical University, Xi'an, Shaanxi 710038, P.R. China, ²Center for Clinical and Translational Science, Mayo Clinic, Rochester, Minnesota 55905, USA, ³Department of Anatomy & K.K. Leung Brain Research Centre, Fourth Military Medical University, Xi'an, Shaanxi, 710032, P.R. China, ⁴Department of Pathology, Tangdu Hospital, Fourth Military Medical University, Xi'an, Shaanxi 710038, P.R. China.

It is highly necessary to identify low versus high risk thymic epithelial tumors (TETs) before operation to guide optimal treatment strategies. Current CT diagnostic parameters could not effectively achieve this goal. We evaluated three parameters of CT scan in a cohort of 216 TETs patients. Parameters of contrast enhancement, risk of aggressiveness, and nodule with fibrous septum were evaluated in low (A, AB) versus high risk (B1, B2, B3 and thymic carcinoma) TETs. Grade of contrast enhancement showed predictive value in classifying low and high risk TETs well. A maximal contrast-enhanced range of 25.5 HU could produce 78.8% sensitivity and 68.5% specificity in determining low risk subtypes. Additionally, risk of aggressiveness parameter was demonstrated to be associated with TETs subtype ($r = 0.801$, $P < 0.001$) and may add confidence in determining low versus high risk subtypes. Furthermore, multiple nodule with fibrous septum could suggest subtype AB. Findings from this study support role of studied parameters of CT manifestations in predicting the low and high risk stages of TETs. These findings provide empirical evidence for incorporating these parameters in clinical practice for identifying TETs stage before operation, if validated in additional studies.

With an incidence of 1.5 cases per million people, thymic epithelial tumors (TETs) account for about 20% of overall mediastinal tumors and 47% of anterior mediastinal tumors¹⁻³. As pathologically classified by The World Health Organization (WHO) in 2004, TETs are now classified as either one of 5 types of thymomas (types A, AB, B1, B2, and B3) or thymic carcinoma⁴. It is shown that the WHO classification could reflect both oncologic behavior and prognostic feature of TETs well^{3,5-7}. Usually type A and AB thymomas are grouped as low risk thymomas with low invasiveness and better prognosis, while type B1, B2 and B3 as high-risk thymomas which are more aggressive⁵. Studies have shown that there are different optimal therapeutic strategies for different stages of TETs⁸⁻¹². For example, in high-risk thymomas and thymic carcinoma patients, adjuvant chemo-radiotherapy is necessary after surgery. Also, at the time of surgery, neo-adjuvant chemo/radio therapy is demonstrated to contribute to a complete resection^{10,11}. Thus an accurate pre-operative identification of the histologic subtype and staging are highly necessary to guide the optimal intervention for TETs patients. However, up to date this objective has not been adequately achieved.

Imaging is very important for the noninvasively preoperative staging and oncological follow up¹³. Computed Tomography (CT) scan is used in the evaluation of majority of TETs cases, which can provide detailed information regarding tumor size, shape, homogeneity and so forth. However, current CT scan cannot effectively differentiate different WHO pathological classifications¹⁴. Although several studies have suggested that CT manifestation parameters (tumor size, shape, necrosis or cystic change, capsule integrity, invasion to the adjacent tissue, lymphadenopathy, the presence of pleural effusion, etc) demonstrated significant differences in different TETs types¹⁴⁻²¹, up to date these parameters could not effectively predict WHO classifications with satisfactory sensitivity and specificity. Besides, the sample sizes of these studies are relatively small, which limits their ability to provide a precise answer for our research question of interest. In a previous pilot study, we proposed a new



parameter of risk of aggressiveness graded by CT, and evaluated its predictive role in 66 TETs patients²². In this study, we conducted a comprehensive retrospective analysis of 216 TETs cases to better characterize the prediction value of this parameter for TETs classifications. Additionally, we evaluated, for the first time, two other new variables of grade of contrast enhancement and multiple nodules with fibrous septum to determine their efficacy in preoperatively differentiating low versus high risk TETs.

Results

General data. Main clinical presentation. A total of 216 patients (130 males and 86 females) with a mean age of 50.0 ± 12.6 were enrolled in this study (Supplementary Table 2). Tumors of the majority of participants (199; 92.1%) were completely resected, and the pathology results of the remaining 17 (7.9%) patients were obtained by core biopsy. According to the histological and immunohistochemical results, from WHO pathological classification perspective there were 11 (5.1%) patients of type A, 47 (21.8%) of type AB, 38 (17.6%) of type B1, 43 (19.9%) of type B2, 21 (9.7%) of type B3, and 56 (25.9%) of thymic carcinoma (Supplementary Table 2).

There was no significant difference in age among different pathological types of thymic tumors ($P > 0.05$), but type B3 thymoma and thymic carcinoma appeared more in males ($P = 0.013$) (Table 1). Among these patients, 51 (23.6%) had no symptoms, especially in patients of types A and AB thymoma (6.55% and 16.34% respectively); 79 (36.5%) were diagnosed with myasthenia gravis (MG), while MG rarely existed in patients of thymic carcinoma (2%); 37 (17.1%) had symptoms of chest tightness and chest pain; and 35 (16.2%) had respiratory symptoms including cough, expectoration, short breath, dyspnea, et al (Table 1).

Distribution of CT Features among patients with different WHO pathological classifications. The distribution of CT features among different WHO classifications were demonstrated in Table 2. Overall, tumor size, boundary, necrosis or cystic change, capsule integrity, homogeneity, the presence of septum, invasion to the adjacent tissue, the presence of pericardiac or pleural effusion, and lymphadenopathy were significantly different among different pathological types of TETs (all $P < 0.001$). Multiple nodules with fibrous septum appeared in 77% of type AB thymomas and were rare in other subtypes. There were no significant differences in shape and calcification between the different pathological types of TETs ($P = 0.206$ and 0.474 , respectively) (Table 2). It seemed that lymphogenous spread was not a common

occurrence in TETs. Lymph node involvement was seen in 3 (1.9%) thymoma patients and in 21 (37.5%) thymic carcinoma patients.

Contrast-enhanced CT features among patients with different WHO pathological classifications. As shown in Table 3, The CE_{max} of types A, AB, B1, B2, and B3 thymic tumors and thymic carcinoma were significantly different. Overall there was significant difference for CE_{max} between low risk (types A, AB) and high risk (B1, B2, B3 and thymic carcinoma) subtypes ($P < 0.001$) (Figure 1). The patterns of contrast enhancement were also significantly different among different pathological types of TETs ($P < 0.001$) (Table 3).

Figure 2 demonstrated the receiver operating characteristic (ROC) curve for the diagnostic performance of the maximal contrast-enhanced range (CE_{max}) in identifying the low from high risk TETs. The area under the curve (AUC) was 0.80 (95% CI, 0.71 to 0.89). And the best cutoff point for CE_{max} is at 25.5 HU, when the sensitivity and specificity for identifying low risk subtypes being 78.8% and 68.5%, respectively (Figure 2).

Relationship between the CT grade of aggressive risk and WHO pathological classifications. As shown in Table 2, for the grade of aggressive risk parameter, 63 (29.2%) patients were categorized in Grade I, 57 (26.4%) in Grade II, 21 (9.7%) in Grade III, and 75 (34.7%) in Grade IV (Table 2). The relationship between different grades of aggressive risk and WHO pathological subtypes was demonstrated in Figure 3. There was a strong correlation between CT grade of aggressive risk and WHO pathological subtypes ($r = 0.801$, $P < 0.001$). Also this parameter could potentially suggest low versus high risk subtypes effectively (Grade I suggested a higher possibility of being low risk subtype, Grade III and IV suggested a higher possibility of being high risk subtype), which might provide additional evidence for subtype prediction. Representative CT images for different grades of aggressive risk were shown in Supplementary Figure 1A–H.

Discussion

The noninvasively preoperative prediction of WHO histologic subtypes is important for guiding treatment strategies for TET patients. Type A and AB thymomas generally behave as a benign tumor and type B1 is a low-grade malignant tumor with the 10-year survival rate being over 90%. Type A, AB, and B1 thymomas usually have more chances of complete resection than other subtypes²³. Type B2 has a greater degree of malignancy, and type B3 shows a poor prognosis, like thymic carcinoma and malignant tumors of other organs⁵.

Table 1 | Clinical and Demographic Characteristics of the Patients

Patient characteristics	A (n = 11)	AB (n = 47)	B1 (n = 38)	B2 (n = 43)	B3 (n = 21)	Thymic carcinoma (n = 56)	P-value
	number (percent)						
Sex							0.013
Males	6(55)	25(53)	17(45)	23(53)	16(76)	43(77)	
Females	5(45)	22(47)	21(55)	20(47)	5(24)	13(23)	
Age							0.466
<45 years	2(18)	17(36)	15(40)	20(46)	5(24)	17(30)	
45–55 years	2(18)	13(28)	10(26)	12(28)	5(24)	14(25)	
>55 years	7(64)	17(36)	13(34)	11(26)	11(52)	25(45)	
Myasthenia gravis							<0.001
Yes	5(45)	21(45)	22(58)	27(63)	3(14)	1(2)	
No	6(55)	26(55)	16(42)	16(37)	16(76)	55(98)	
Symptoms							<0.001*
No symptom	6(55)	16(34)	9(23)	9(21)	2(10)	9(16)	
Myasthenia	5(45)	21(45)	22(58)	27(63)	3(14)	1(2)	
Chest pain	—	1(2)	3(8)	1(2)	7(33)	25(45)	
Respiratory symptoms	—	7(15)	3(8)	5(12)	7(33)	13(23)	
Others	—	2(4)	1(3)	1(2)	2(10)	8(14)	

*P-values were calculated by Monte Carlo Test.



Table 2 | Relationship between CT findings and WHO histologic subtypes

Variable	A (n = 11)	AB (n = 47)	B1 (n = 38)	B2 (n = 43)	B3 (n = 21)	Thymic Carcinoma (n = 56)	P-value
Size							
Maximum diameter - no. (%)							0.000
<4	4(36)	15(32)	20(53)	24(56)	8(38)	11(20)	
4–8	6(55)	18(38)	15(40)	15(35)	8(38)	19(34)	
>8	1(9)	14(30)	3(8)	4(9)	5(24)	26(46)	
Mean diameter (mean ± sd; cm)	3.97 ± 2.37	5.52 ± 2.47	4.36 ± 1.78	3.95 ± 1.73	5.27 ± 2.68	6.00 ± 2.31	0.000*
Shape- no. (%)							
Round	6(55)	20(42)	14(37)	16(37)	9(43)	22(39)	
Oval	5(45)	23(49)	16(42)	18(42)	5(24)	18(32)	
Irregular	—	4(9)	8(21)	9(21)	7(33)	16(29)	
Boundary- no. (%)							
Smooth	8(73)	12(25)	9(24)	—	—	—	0.000
Lobulated	3(27)	30(64)	19(50)	29(67)	4(19)	8(14)	
Irregular	—	5(11)	10(26)	14(33)	17(81)	48(86)	
Capsule integrity - no. (%)							
Almost complete	11(100)	31(66)	13(34)	8(19)	—	1(2)	0.000
Partial	—	16(34)	25(66)	35(81)	21(100)	55(98)	
Homogeneity- no. (%)							
Homogeneous	9(82)	24(51)	15(40)	23(53)	7(33)	14(25)	0.002
Heterogeneous	2(18)	23(49)	23(61)	20(47)	14(67)	42(75)	
Septum - no. (%)							
Yes	2(18)	36(77)	5(13)	2(5)	1(5)	—	0.000
No	9(82)	11(23)	33(87)	41(95)	20(95)	56(100)	
Calcification - no. (%)							
Yes	1(9)	12(26)	13(34)	11(26)	8(38)	19(34)	0.474
No	10(91)	35(74)	25(66)	32(74)	13(62)	37(66)	
Necrotic or cystic change - no. (%)							
Yes	1(9)	14(30)	16(42)	15(35)	10(48)	39(70)	0.000
No	10(91)	33(70)	22(58)	28(65)	11(52)	17(30)	
Pericardiac or Pleural effusion - no. (%)							
Yes	—	1(2)	4(11)	12(28)	12(57)	49(88)	0.000
No	11(100)	46(98)	34(89)	31(72)	9(43)	7(12)	
Lymphadenopathy - no. (%)							
Yes	—	—	—	2(5)	1(5)	21(37)	0.000†
No	11(100)	47(100)	38(100)	41(95)	20(95)	35(63)	
Involvement of adjacent tissues - no. (%)							
Yes	—	—	6(16)	15(35)	19(90)	55(98)	0.000
No	11(100)	47(100)	32(84)	28(65)	2(10)	1(2)	
Grade of aggressive risk by CT - no. (%)							
Grade I	11(100)	31(66)	13(34)	8(19)	—	—	
Grade II	—	15(32)	19(50)	20(46)	2(10)	1(2)	
Grade III	—	1(2)	2(5)	4(9)	7(33)	7(12)	
Grade IV	—	—	4(11)	11(26)	12(57)	48(86)	

*P-values were calculated by ANOVA;
†P-values were calculated by Monte Carlo Test.

Table 3 | Relationship between patterns of contrast-enhancement and WHO histologic subtypes

Variable	A (n = 7)	AB (n = 26)	B1 (n = 22)	B2 (n = 24)	B3 (n = 15)	Thymic Carcinoma (n = 47)	P-value
CE _{max}							
Mean ± sd(HU)	41.1 ± 15.8 ^a	33.0 ± 9.6 ^b	23.0 ± 8.7 ^c	22.0 ± 8.2 ^c	20.9 ± 9.5 ^c	23.6 ± 9.1 ^c	0.000*
Pattern of CE - no. (%)							0.000†
Mild	—	2(8)	10(45.5)	14(58)	8(53)	16(34)	
Moderate	3(43)	15(57)	10(45.5)	9(38)	6(40)	29(62)	
Strong	4(57)	9(35)	2(9)	1(4)	1(7)	2(4)	

*P-values were calculated by one-way ANOVA; the different alphabet represented a significant difference between the two groups;
†P-values were calculated by Monte Carlo Test.
CE_{max}: maximal contrast-enhanced range; CE: contrast enhancement.

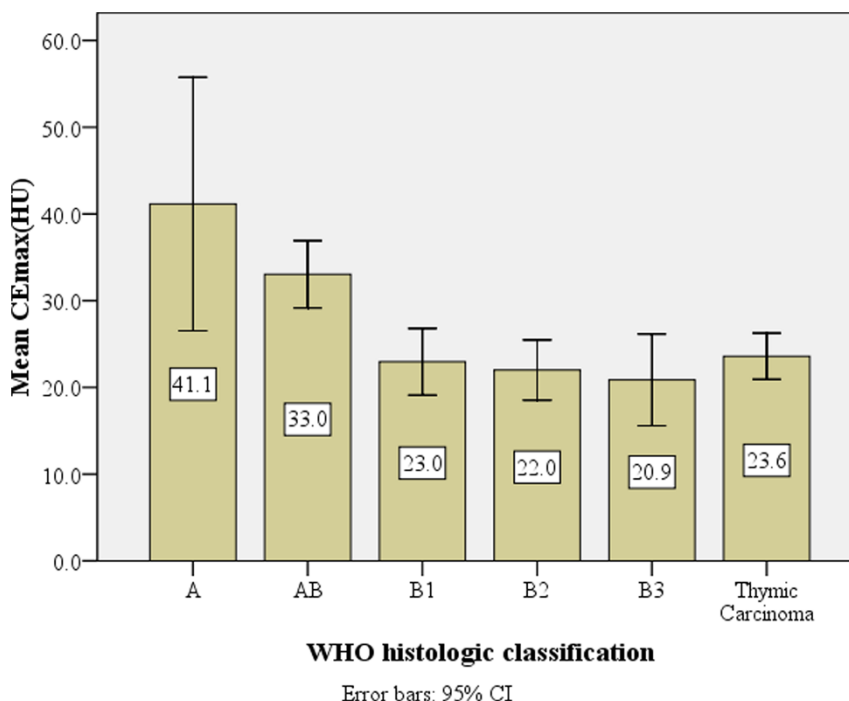
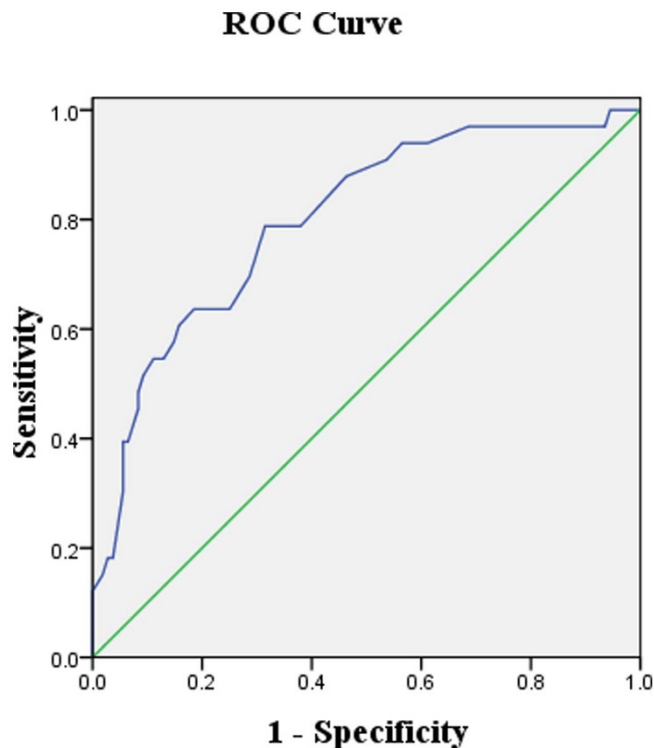


Figure 1 | The relationship between mean CE_{max} value (HU) and the WHO pathological classification of thymic epithelial tumors.



Diagonal segments are produced by ties.

Figure 2 | The receiver-operating-characteristic (ROC) curve describing the diagnostic performance of the maximal contrast-enhanced range (CE_{max}) to identify the low risk (A, AB) from high risk (B1, B2, B3 and thymic carcinoma) subtypes of TETs.

Patients with type B2 or B3 thymomas, or thymic carcinoma might require adjuvant chemo-radiotherapy²³.

In this study, we employed the largest cohort of TETs patients up to date to investigate whether CT diagnostic parameters could identify staging of this cancer. The conventional CT findings can determine tumor size, shape, density, involvement of the capsule and surrounding tissues, all of which are related to the WHO histologic classification and clinical stages of TETs. In our study, a greater average tumor diameter indicates a higher probability that the tumor is malignant. It is very often for thymic carcinoma to have a maximum diameter of larger than 8 cm (49.1%). Low risk thymic tumors (types A, AB) are often round or oval with a clear, smooth margin, complete capsule and homogenous density; on the contrary, high risk subtypes (types B1, B2, B3 and thymic carcinoma) are often irregular in shape or deep lobulated. There is usually a higher rate of invasion by direct extending to adjacent structures including pericardium, large vessels or lung. The lobulation rate is between 60% and 89% based on previous study²³. Focusing on common CT manifestation parameters, we detected that size, boundary, capsule, homogeneity, septa, necrotic or cystic change, pleural effusion, lymphadenopathy, and invasion of adjacent tissues demonstrated significant differences among the 6 TETs subtypes, which confirms previous findings^{14–18}. However, there was no significant difference for tumor shape among the different pathological types of TETs ($P = 0.206$), which is inconsistent with previous studies^{14–18}. The finding that there was no significant difference for calcification among the different pathological types of TETs ($P = 0.474$) confirms the conclusion from a previous systematic review²⁴.

CT enhancement is very often used in TETs diagnosis since it can better reveal the tumor shape and invasion to adjacent tissues, as well as demonstrate the blood supply to tumor tissues. For the first time, we demonstrated that significantly different degrees of CT enhancement exist for different TETs WHO classifications. The area under the ROC curve for differentiating low (types A, AB) from high risk subtypes (types B1, B2, B3 and thymic carcinoma) reaches 80%. And the best cutting point for CE_{max} is at 25.5 HU, when the sensitivity and specificity of determining low risk subtypes are 78.8% and 68.5%, respectively. Generally speaking, degree of CT enhancement may

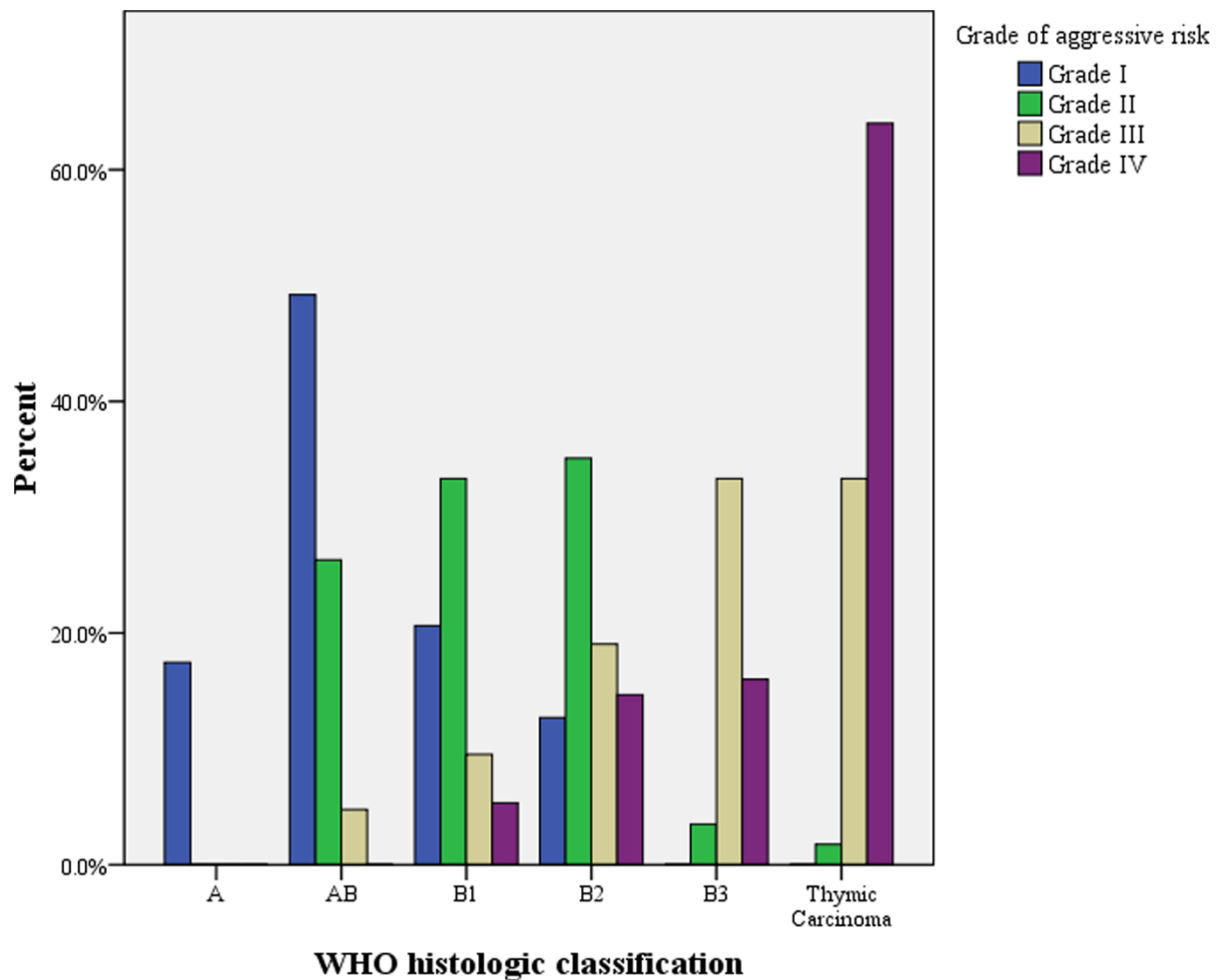


Figure 3 | The relationship between mean grade of aggressive risk and the WHO pathological classification of thymic epithelial tumors.

represent levels of blood supply, thus should increase with more advanced tumor stages. Research has indicated a significant correlation between tumor angiogenesis and invasiveness in patients with TETs²⁵. However, our finding is out of expectation in suggesting that low risk subtype of thymoma (type A and AB) demonstrated a high degree of CT enhancement while high risk ones demonstrated a much lower degree of CT enhancement. Pan et al studied the clinicopathologic characteristics of spindle cell thymoma (medullary, WHO type A) and mixed spindle/lymphocytic thymoma (WHO type AB), and found that the short-spindled pattern of type A thymoma may commonly arrange in a hemangiopericytic or microcystic pattern²⁶, which may explain why a higher degree of CT enhancement exist in low risk subtypes in our study. To the best of our knowledge, this exploration of degree of CT enhancement and stage of TETs has never been investigated before, and focusing on our clinical question itself, this interesting finding implies that degree of CT enhancement can probably predict the classifications of TETs.

The Masaoka staging system has been widely used in the clinical management of TETs with the clinical stage remaining the most important prognostic factor of thymoma^{5,27}. A recent study demonstrated a close relationship between preoperative CT thymoma staging and postoperative Masaoka clinical staging²⁸. Based on CT demonstrations of pathological classifications and Masaoka stages of primary mediastinal tumor, we proposed a parameter of aggressive risk. In this comprehensive analysis of 216 TETs patients, we detected a strong correlation between CT grade of aggressive risk and WHO histological classification ($r = 0.801, P < 0.001$). Our data also suggested that such a parameter could potentially help differ-

entiate low from high risk TET subtypes, which could potentially add confidence in such a determination besides the parameter of degree of CT enhancement.

Interestingly, in our study we detected that multiple nodule with fibrous septum appeared in over 77% of type AB thymomas, but was rare in other subtypes and if existed, with a different manifestation. Histologically, type AB thymoma showed multiple nodules separated by fibrous bands⁴. The multiple nodules with fibrous septum features on CT imaging are consistent with the macroscopic appearance of a type AB thymoma (Supplementary Fig 2A)²⁶. However, high risk TET subtypes especially thymic carcinoma appear as mainly deep lobulation or spiculate protuberance without tumor septum (Supplementary Fig 2B). This finding is useful in determining type AB thymomas. The detection of tumor septum can potentially be useful as a marker for type AB thymoma.

Our study also has limitations to acknowledge. Firstly, we did not analyze CT characteristics of thymic carcinoma according to their specific pathological classifications. Certain subtypes of thymic carcinoma such as neuroendocrine carcinomas have differentiated CT manifestations and prognosis, which warrants further study. Secondly, the complete survival data of these patients are not available, which intimidates the possibility to determine the relationship between survival and variables of risk of aggressiveness and degree of CT enhancement. The fact that survival rates of TETs patients, especially for those in low risk subgroups, are relatively high and a very long follow up will be required to collect these data. Further study for elucidating this research question is warranted. Thirdly, the hemodynamic analysis of TETs based on histopathology was not con-



ducted, and further study for resolving this research question will be needed to clarify the mechanism of CT enhancement finding in this study.

In conclusion, using the largest sample up to date, we identified that several variables which are largely unreported before, including degree of CT enhancement, risk of aggressiveness, and multiple nodule with fibrous septum could preoperatively help determine the WHO pathological classification of TETs patients, especially for the low risk and high risk subtypes. A combined prediction using these variables will provide a better guidance for appropriate therapeutic strategies for TETs patients.

Methods

Participants. Between February 2009 and March 2014, 216 patients of TETs were sequentially enrolled in Tangdu Hospital, whose diseases were further confirmed by surgical pathology or needle biopsy. Plain CT scan was performed on all 216 patients, among which contrast-enhanced CT scan was further performed on 141 patients. All plain and enhanced CT data were available, combined with histological and immunohistochemical examinations for WHO pathological classification. Demographic data and clinical symptoms were also collected. This study was conducted in accordance with the declaration of Helsinki. This study was approved by Ethics Committee of Tangdu Hospital of the Fourth Military Medical University, and informed consent was waived.

Image Acquisition and Analysis. Philips 256-slice CT (Brilliance iCT, Philips Healthcare, Cleveland, USA), GE 64-slice CT (GE-Medical-Systems, Milwaukee, USA) and Siemens 16-slice CT (Somatom Sensation, Siemens, Erlangen, Germany) were used. In all patients, the scan range for plain CT was from the thoracic inlet to the diaphragmatic level. The slice thickness and interval were each 5 mm. Other scanning parameters were 120 kV and 200 mAs. Before the CT scanning, patients were instructed to hold their breath to avoid motion artifacts. Dual-phase arterial and venous enhanced CT was performed in a proportion of patients after obtaining their agreement. A total of 40 to 120 mL (1.5 mL/kg weight) of contrast medium (Ultravist, Schering Pharmaceutical Ltd, Guangzhou, 300 mg/mL) were injected by using a power injector at a rate of 3.0 mL/s. Scanning parameters were same as plain CT. All imaging data underwent further multi-planar reconstruction and were analyzed at medical imaging workstation.

Two senior radiologists reviewed the imaging data, according to the recommendation of the Nomenclature Committee of the Fleischner Society²⁹. They were told before the review that the patients had thymic epithelial tumors, but they were blinded to the specific pathological classifications. Decisions regarding the CT findings were reached by consensus. All monitors showed images obtained using both mediastinal (width, 320 Hounsfield Units (HU); level, 35 HU) and lung (width, 1000 HU; level, -600 HU) window settings.

CT imaging features of TETs were assessed for the following parameters: 1) Shape and boundary: the tumor shape was evaluated based on the ratio of the long axis diameter to the short axis diameter. It was classified as round if the long- to short-axis ratio was less than or equal to 1.5, oval if the ratio was greater than 1.5 but less than 2.0, or irregular if the ratio was greater than or equal to 2.0. Marginal characteristics were subclassified as smooth, lobulated, or irregular; 2) Size: the longest diameter of the tumor was measured where the tumor appeared largest on an axial image. Based on this, tumors were divided into three groups: ≤ 4.0 cm, 4.0 ~ 8.0 cm, and ≥ 8.0 cm. The mean diameter (D_{mean}) was calculated by $D_{\text{mean}} = (a + b + c)/3$, and the maximal cross-section was used to measure the long and short diameters; 3) Homogeneity: with a standard mediastinal window setting, areas with a CT value difference less than 10 HU represented homogeneity, otherwise represented heterogeneity. The presences of calcification, necrosis or cystic change were also evaluated; 4) Capsule integrity: almost complete (smooth or shadow lobulation), partial complete (deep lobulation or spiculate protuberance); 5) Involvement of adjacent tissues: mediastinal fat layer of peritumour (clear, blurred, or disappeared), pleura and pericardium (irregular interface with an absent space between tumor and pleura or pericardium; thickening; effusion); Mediastinal blood vessels (absent space between tumor and blood vessels; oppression, deformation and occlusion of vessels; tumor thrombus in the vessels; tumor capsulating $> 1/4$ circumference of vessel); 6) Lymph node enlargement: A measurement of the shortest lymph node diameter > 1.0 cm was defined as lymph node enlargement; 7) Pattern of contrast enhancement: a maximal difference of CT values between plain scan and contrast-enhancement phase in the solid component of tumor, which is denoted as maximal contrast-enhanced range (CE_{max}). This parameter was divided into three groups of mild, moderate and strong contrast enhancement, with indication of $CE_{\text{max}} \leq 20.0$ HU, 20.0–40.0 HU, and ≥ 40.0 HU, respectively; Region of interests (ROIs) should not be near superior vena cava which is strong contrast enhancement evident, and should not be areas of fringe, calcification or necrotic. The ROIs should be uniform, thus the sizes should be relatively homogeneous. To avoid quantum noise, ROIs should be no less than 50 pixels, and be like round shape. Depending on actual situation, size of ROIs can be small if lesion is relatively small; when lesion is relatively large, several ROIs with the same size can be selected and the average number is calculated; 8) Risk of aggressiveness: This 4-grade system of aggressive risk is based on CT findings of

TETs subtypes and Masaoka stages of primary mediastinal tumors^{3,30} (Supplementary Table 1).

Statistical analysis. Numerical variables were denoted as mean and standard deviation. The between-group comparisons of gender, age, and CT manifestations (including tumor size, shape, boundary, homogeneity, calcification, necrosis or cystic change, capsular integrity, tumor septum, invasion to the adjacent tissue, the presence of pericardiac or pleural effusion, and lymphadenopathy) were conducted using the chi-square test or Fisher's exact test. The between-group comparisons of D_{mean} and CE_{max} values were conducted using ANOVA test. Spearman correlation analyses were conducted to determine the correlation between the grade of aggressive risk and WHO pathology subtypes of TETs. ROC analyses were performed to determine optimum thresholds for differentiating the low risk and the high risk TETs by CE_{max} value and to calculate the sensitivity, specificity, and area under curve (AUC) for identifying low risk thymoma. $P < 0.05$ indicated a statistically significant difference. SPSS17.0 software (SPSS Inc, Chicago, IL, USA) was used for statistical analyses.

- Engels, E. A. Epidemiology of thymoma and associated malignancies. *J Thorac Oncol* **5**, S260–265, doi:10.1097/JTO.0b013e3181f162d (2010).
- Engels, E. A. & Pfeiffer, R. M. Malignant thymoma in the United States: demographic patterns in incidence and associations with subsequent malignancies. *Int J Cancer* **105**, 546–551, doi:10.1002/ijc.11099 (2003).
- Chen, G. *et al.* New WHO histologic classification predicts prognosis of thymic epithelial tumors: a clinicopathologic study of 200 thymoma cases from China. *Cancer* **95**, 420–429, doi:10.1002/cncr.10665 (2002).
- Travis, W. D. B. E., Müller-Hermelink, H. K. & Harris, C. C. *World Health Organization Classification of Tumours. Pathology and Genetics of Tumours of the Lung, Pleura, Thymus and Heart* (IARC Press, 2004).
- Okumura, M. *et al.* The World Health Organization histologic classification system reflects the oncologic behavior of thymoma: a clinical study of 273 patients. *Cancer* **94**, 624–632 (2002).
- Kondo, K. *et al.* WHO histologic classification is a prognostic indicator in thymoma. *Ann Thorac Surg* **77**, 1183–1188, doi:10.1016/j.athoracsurg.2003.07.042 (2004).
- Honglin, Y. *et al.* The correlation of the World Health Organization histologic classification of thymic epithelial tumors and its prognosis: a clinicopathologic study of 108 patients from China. *Int J Surg Pathol* **17**, 255–261, doi:10.1177/1066896909334126 (2009).
- Lococo, F. *et al.* Role of combined 18F-FDG-PET/CT for predicting the WHO malignancy grade of thymic epithelial tumors: a multicenter analysis. *Lung Cancer* **82**, 245–251, doi:10.1016/j.lungcan.2013.08.003 (2013).
- Viti, A., Terzi, A., Bianchi, A. & Bertolaccini, L. Is a positron emission tomography-computed tomography scan useful in the staging of thymic epithelial neoplasms? *Interact Cardiovasc Thorac Surg*, doi:10.1093/icvts/ivu068 (2014).
- Sung, Y. M. *et al.* 18F-FDG PET/CT of thymic epithelial tumors: usefulness for distinguishing and staging tumor subgroups. *J Nucl Med* **47**, 1628–1634 (2006).
- Rea, F. *et al.* Long-term survival and prognostic factors in thymic epithelial tumours. *Eur J Cardiothorac Surg* **26**, 412–418, doi:10.1016/j.ejcts.2004.04.041 (2004).
- Casey, E. M., Kiel, P. J. & Loehrer, P. J., Sr. Clinical management of thymoma patients. *Hematol Oncol Clin North Am* **22**, 457–473, doi:10.1016/j.hoc.2008.03.010 (2008).
- Marom, E. M. Advances in thymoma imaging. *J Thorac Imaging* **28**, 69–80; quiz 81–63, doi:10.1097/RTI.0b013e31828609a0 (2013).
- Tomiya, N. *et al.* Using the World Health Organization Classification of thymic epithelial neoplasms to describe CT findings. *AJR Am J Roentgenol* **179**, 881–886, doi:10.2214/ajr.179.4.1790881 (2002).
- Han, J. *et al.* Thymic epithelial tumors classified according to a newly established WHO scheme: CT and MR findings. *Korean J Radiol* **4**, 46–53 (2003).
- Sadohara, J. *et al.* Thymic epithelial tumors: comparison of CT and MR imaging findings of low-risk thymomas, high-risk thymomas, and thymic carcinomas. *Eur J Radiol* **60**, 70–79, doi:10.1016/j.ejrad.2006.05.003 (2006).
- Jeong, Y. J. *et al.* Does CT of thymic epithelial tumors enable us to differentiate histologic subtypes and predict prognosis? *AJR Am J Roentgenol* **183**, 283–289, doi:10.2214/ajr.183.2.1830283 (2004).
- Liu, G. B. *et al.* Relationship between computed tomography manifestations of thymic epithelial tumors and the WHO pathological classification. *Asian Pac J Cancer Prev* **13**, 5581–5585 (2012).
- Qu, Y. J. *et al.* Preoperative CT findings of thymoma are correlated with postoperative Masaoka clinical stage. *Acad Radiol* **20**, 66–72, doi:10.1016/j.acra.2012.08.002 (2013).
- Tomiya, N. *et al.* Invasive and noninvasive thymoma: distinctive CT features. *J Comput Assist Tomogr* **25**, 388–393 (2001).
- Priola, A. M. *et al.* Computed tomography and thymoma: distinctive findings in invasive and noninvasive thymoma and predictive features of recurrence. *Radiol Med* **115**, 1–21, doi:10.1007/s11547-009-0478-3 (2010).
- Hu, Y. C. M. F., Zhang, B., Li, G. F., Yu, Y. & Cui, G. B. Relationship between WHO pathology subtypes and CT features of thymic epithelial tumors. *Radiologic Practice* **29**, 404–407 (2014).



23. Tomiyama, N. *et al.* Using the World Health Organization Classification of thymic epithelial neoplasms to describe CT findings. *AJR Am J Roentgenol* **179**, 881–886, doi:10.2214/ajr.179.4.1790881 (2002).
24. Harris, K., Elsayegh, D., Azab, B., Alkaied, H. & Chalhoub, M. Thymoma calcification: is it clinically meaningful? *World J Surg Oncol* **9**, 95, doi:10.1186/1477-7819-9-95 (2011).
25. Tomita, M. *et al.* Correlation between tumor angiogenesis and invasiveness in thymic epithelial tumors. *J Thorac Cardiovasc Surg* **124**, 493–498 (2002).
26. Pan, C. C., Chen, W. Y. & Chiang, H. Spindle cell and mixed spindle/lymphocytic thymomas: an integrated clinicopathologic and immunohistochemical study of 81 cases. *Am J Surg Pathol* **25**, 111–120 (2001).
27. Rios, A. *et al.* Prognostic factors in thymic epithelial neoplasms. *Eur J Cardiothorac Surg* **21**, 307–313 (2002).
28. Qu, Y. J. *et al.* Preoperative CT findings of thymoma are correlated with postoperative Masaoka clinical stage. *Acad Radiol* **20**, 66–72, doi:10.1016/j.acra.2012.08.002 (2013).
29. Hansell, D. M. *et al.* Fleischner Society: glossary of terms for thoracic imaging. *Radiology* **246**, 697–722, doi:10.1148/radiol.2462070712 (2008).
30. Weissferdt, A. & Moran, C. A. Staging of primary mediastinal tumors. *Adv Anat Pathol* **20**, 1–9, doi:10.1097/PAP.0b013e31827b6619 (2013).

Acknowledgments

We thank other consultants of Department of Radiology of Tangdu hospital for their help in this study. We also thank Tangdu hospital for providing related instruments for this study. Gratitude is also extended to Scientific and Technological Development Program of

Shaanxi Province (2012K13-02-27) and Tangdu Hospital of Fourth Military Medical University for funding support for this study.

Author contributions

G.-B.C. conceived the study. Y.-C.H. and L.W. participated in the study design. Y.-C.H., L.-F.Y., S.-M.W., B.-Y.C., G.-F.L. and B.Z. performed the data acquisition. Y.-C.H., L.W. and W.W. participated in the statistical analyses. All authors participated in the data interpretation. Y.-C.H. and L.W. drafted the first version of the report. All authors revised and approved the final draft of the report.

Additional information

Supplementary Information accompanies this paper at <http://www.nature.com/scientificreports>

Competing financial interests: The authors declare no conflicts of interest.

How to cite this article: Hu, Y.-C. *et al.* Predicting Subtypes of Thymic Epithelial Tumors Using CT: New Perspective based on a Comprehensive Analysis of 216 Patients. *Sci. Rep.* **4**, 6984; DOI:10.1038/srep06984 (2014).



This work is licensed under a Creative Commons Attribution-NonCommercial-ShareAlike 4.0 International License. The images or other third party material in this article are included in the article's Creative Commons license, unless indicated otherwise in the credit line; if the material is not included under the Creative Commons license, users will need to obtain permission from the license holder in order to reproduce the material. To view a copy of this license, visit <http://creativecommons.org/licenses/by-nc-sa/4.0/>